CHARACTERISTICS OF c-C_4F_8, c-C_4F_8/Ar, O_2 INDUCTIVELY COUPLED PLASMAS FOR DIELECTRIC ETCHING[1]

Alex V. Vasenkov[2], Gottlieb S. Oehrlein[3] and Mark J. Kushner[2]

[2]University of Illinois
Department of Electrical and Computer Engineering
Urbana, IL 61801

[3]University of Maryland, Materials Science and Engineering & Institute for Research in Electronics and Applied Physics
College Park, MD 20742-2115

E-mail: vasenkov@uiuc.edu
oehrlein@glue.umd.edu
mjk@uiuc.edu

November 2002

[1]Work supported by CFD Research Corp., NSF,
Applied Materials, Inc. and the SRC

AGENDA

- Magnetically enhanced ICPs
- Description of the model
- Ar/C_4F_8 and O_2 reaction mechanisms
- Validation of the mechanisms for ICPs in Ar, O_2 and C_4F_8
- Static magnetic fields and ICPs
- Summary

University of Illinois
Optical and Discharge Physics

MAGNETICALLY ENHANCED ICPs

- ICPs are the workhorse of the microelectronics industry for etching of materials.
- To obtain higher ionization efficiencies magnetically enhanced ICP (MEICP) sources have been proposed to replace conventional ICP sources.
- The mechanisms for these high efficiencies are not well understood.
- This presentation reports on a computational study of MEICPs in Ar/C_4F_8 which are used for selective plasma etching.

FLUORCARBON PLASMA ETCHING: SELECTIVITY

$$e + Ar/C_4F_8 \longrightarrow CF_n, M^+$$

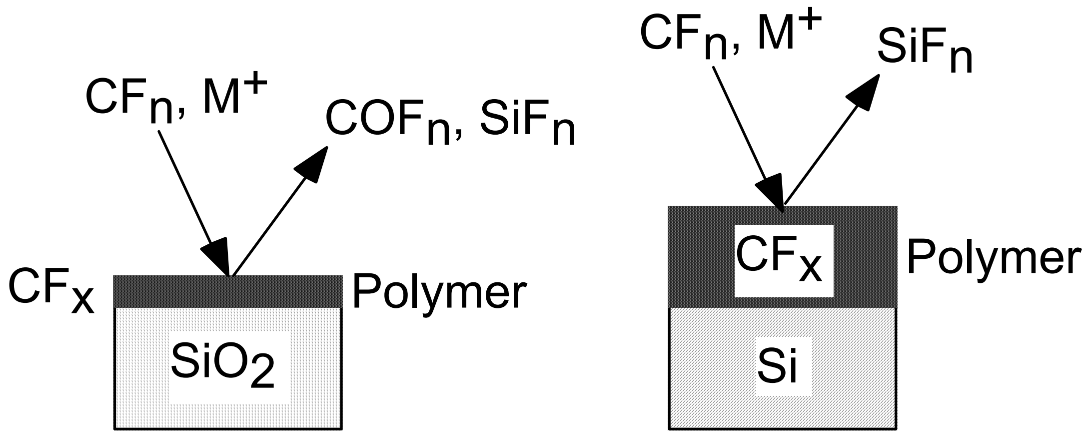

- **Electron impact dissociation of feedstock fluorocarbons produce polymerizing radicals and ions; resulting in polymer deposition.**
- **Selectivity in fluorocarbon etching relies on this polymer deposition.**
- **O_2 is used to control degree of polymerization.**

University of Illinois
Optical and Discharge Physics

HYBRID PLASMA EQUIPMENT MODEL

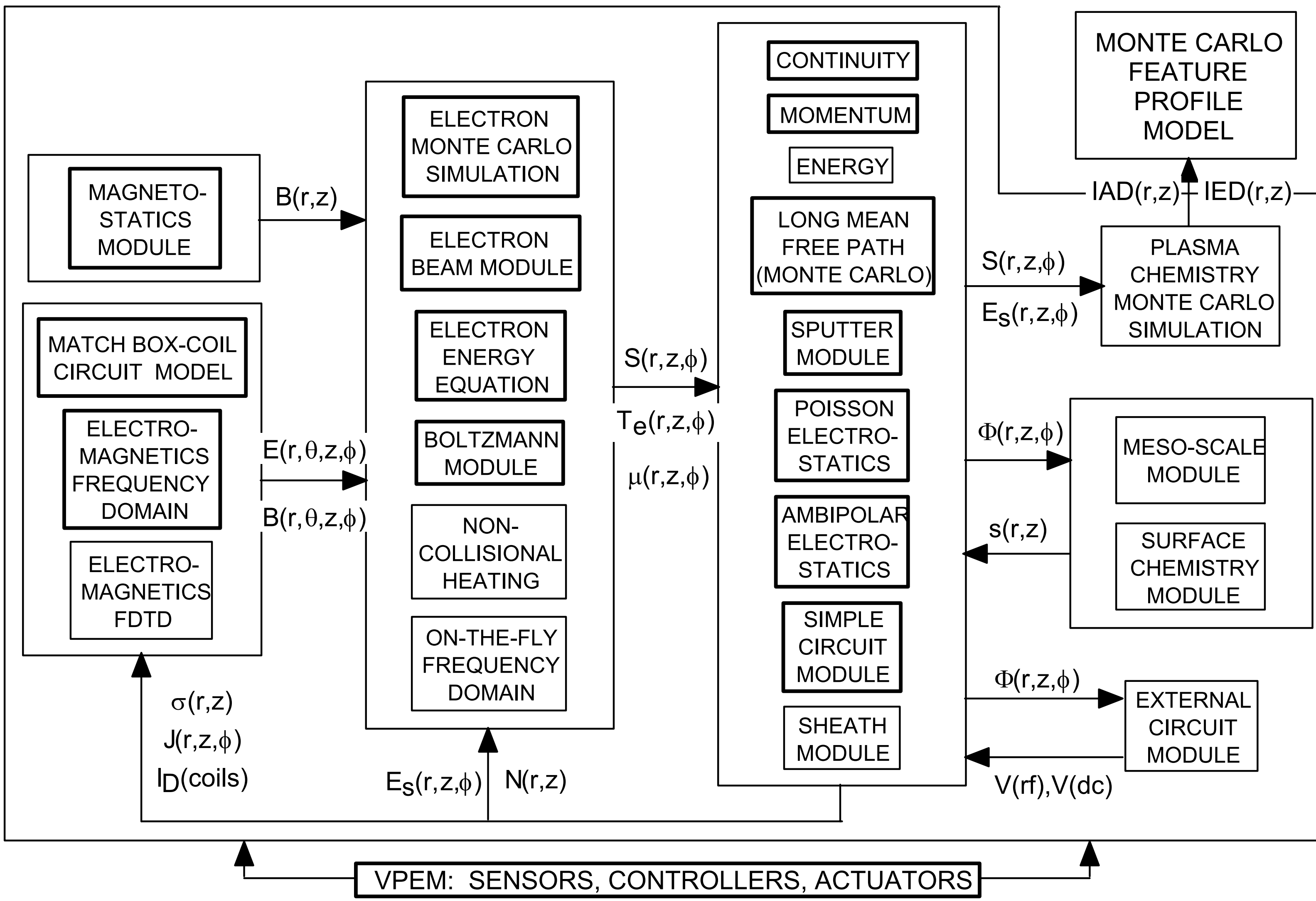

University of Illinois
Optical and Discharge Physics

ELECTROMAGNETICS MODEL

- **The wave equation is solved in the frequency domain using sparse matrix techniques (2D,3D):**

$$-\nabla\left(\frac{1}{\mu}\nabla\cdot\overline{E}\right)+\nabla\cdot\left(\frac{1}{\mu}\nabla\overline{E}\right)=\frac{\partial^2\left(\varepsilon\overline{E}\right)}{\partial t^2}+\frac{\partial\left(\overline{\overline{\sigma}}\cdot\overline{E}+\overline{J}\right)}{\partial t}$$

$$\vec{E}(\vec{r},t)=\vec{E}'(\vec{r})\exp(-i(\omega t+\varphi(\vec{r})))$$

- **Conductivities are tensor quantities (2D,3D):**

$$\overline{\overline{\sigma}}=\sigma_o\frac{m\nu_m}{q\alpha}\frac{1}{\left(\alpha^2+\left|\vec{B}\right|^2\right)}\begin{pmatrix}\alpha^2+B_r^2 & \alpha B_z+B_rB_\theta & -\alpha B_\theta+B_rB_z\\ -\alpha B_z+B_rB_\theta & \alpha^2+B_\theta^2 & \alpha B_r+B_\theta B_z\\ -\alpha B_\theta+B_rB_z & -\alpha B_r+B_\theta B_z & \alpha^2+B_z^2\end{pmatrix}$$

$$\vec{j}=\overline{\overline{\sigma}}\cdot\vec{E} \qquad \alpha=\frac{\left(i\omega+\nu_m\right)}{q/m},\quad \sigma_o=\frac{q^2n_e}{m\nu_m}$$

University of Illinois
Optical and Discharge Physics

Ar/C_4F_8 REACTION MECHANISMS

- **The limited electron impact cross-section data for the fluorocarbon species were collected and synthesized.**

- **Rate coefficients for gas phase chemistry were taken from independent studies in the literature or estimated from measurements for related species.**

- **The mechanisms were validated by comparing to measured ion saturation currents obtained with probes and ion spectra measurements.**

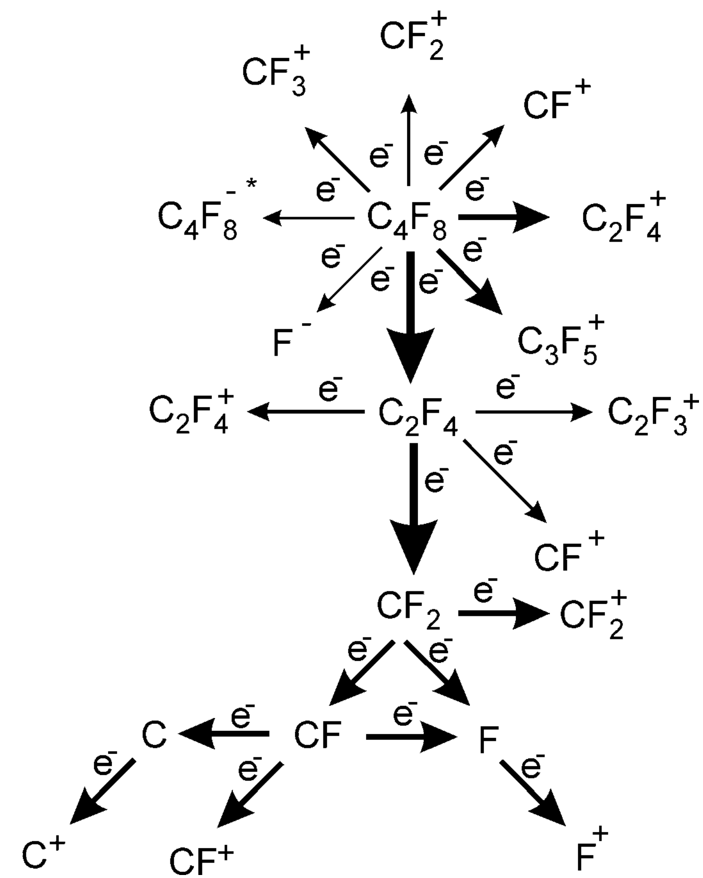

University of Illinois
Optical and Discharge Physics

ICP CELL FOR VALIDATION AND INVESTIGATION

- **An ICP reactor patterned after Oeherlein, et al. was used for validation.**
- **Reactor uses a metal ring with magnets to confine plasma.**

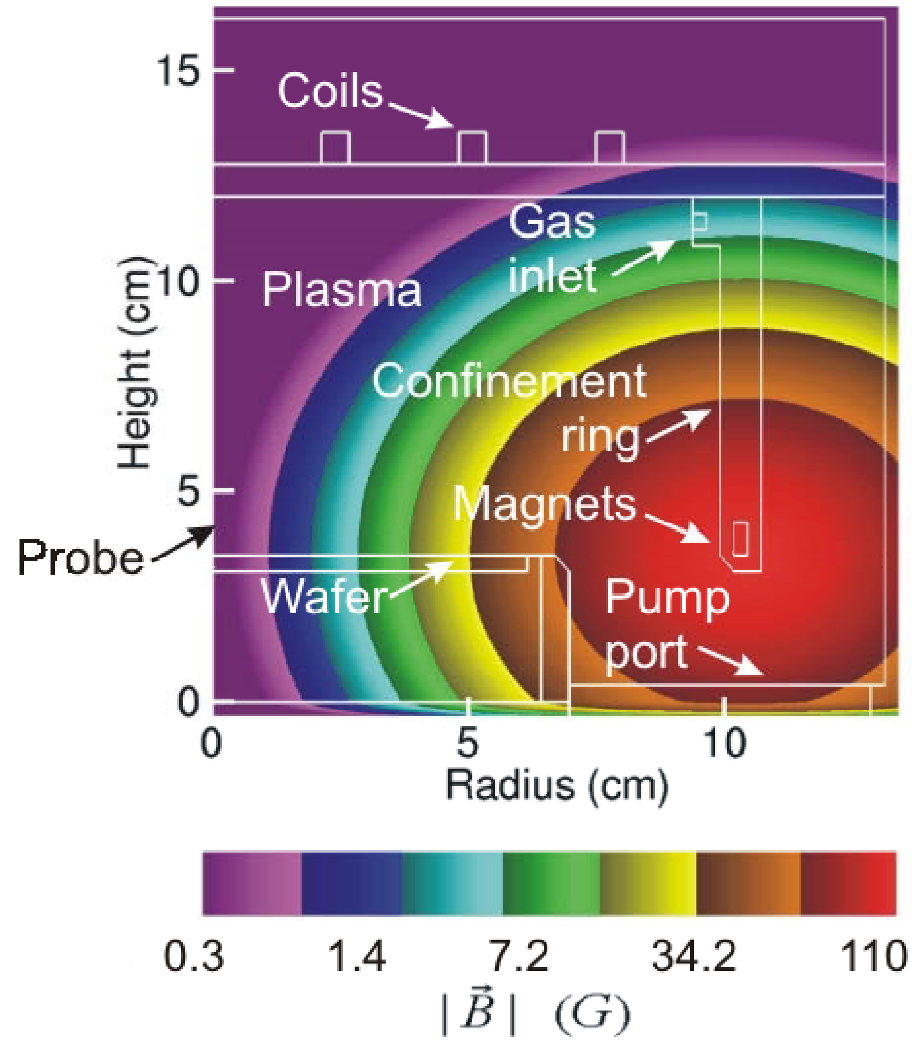

University of Illinois
Optical and Discharge Physics

ELECTRON DENSITY FOR BASE CASE

- **Electron density is largest in the middle of reactor where the electric potential is maximum.**

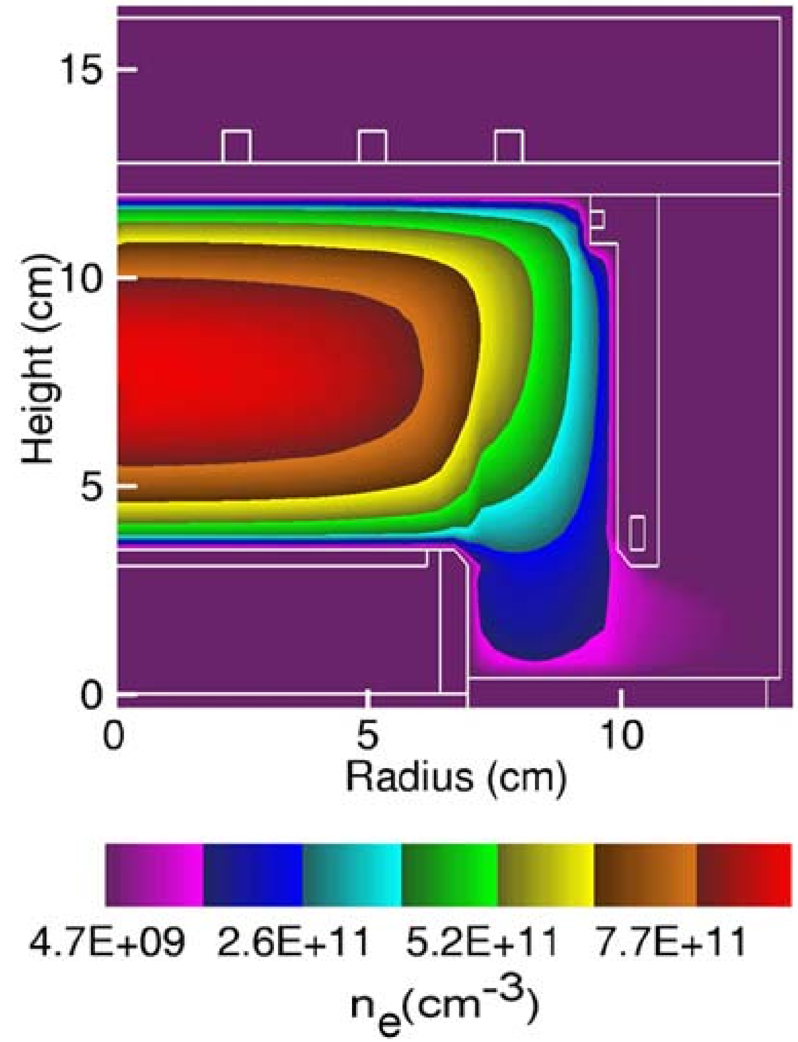

- **C_4F_8, 10 mTorr, 1.4 kW, 13.56 MHz**

University of Illinois
Optical and Discharge Physics

CF_2^+ DENSITY FOR BASE CASE

- CF_2^+ is one of the dominant ions in C_4F_8 plasmas due to large dissociation.
- The major path for the CF_2^+ is:
- $C_4F_8 + e \rightarrow C_2F_4 + C_2F_4 + e$
- $C_2F_4 + e \rightarrow CF_2 + CF_2 + e$
- $CF_2 + e \rightarrow CF_2^+ + e + e$

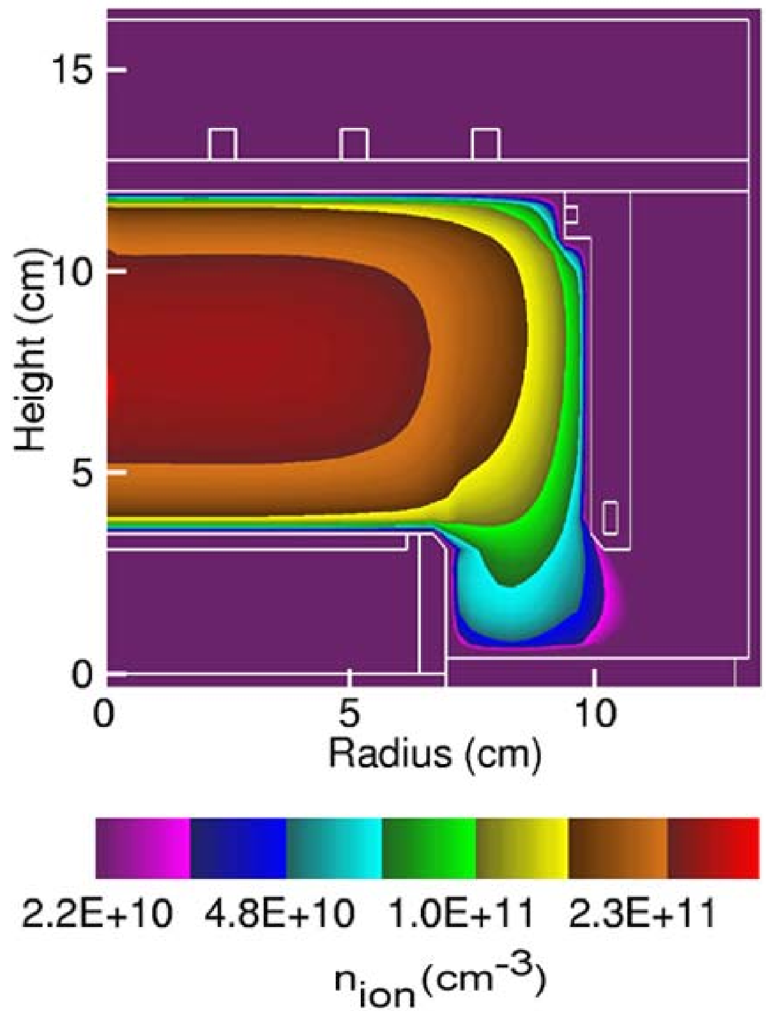

- C_4F_8, 10 mTorr, 1.4 kW, 13.56 MHz

University of Illinois
Optical and Discharge Physics

ELECTRON TEMPERATURE FOR BASE CASE

- The peak in electron temperature occurs in the skin layer due to the collisionless electron heating by the large electric field.
- The electron temperature is rather uniform over the radius in the bulk plasma where electrons experience a large number of e-e collisions.

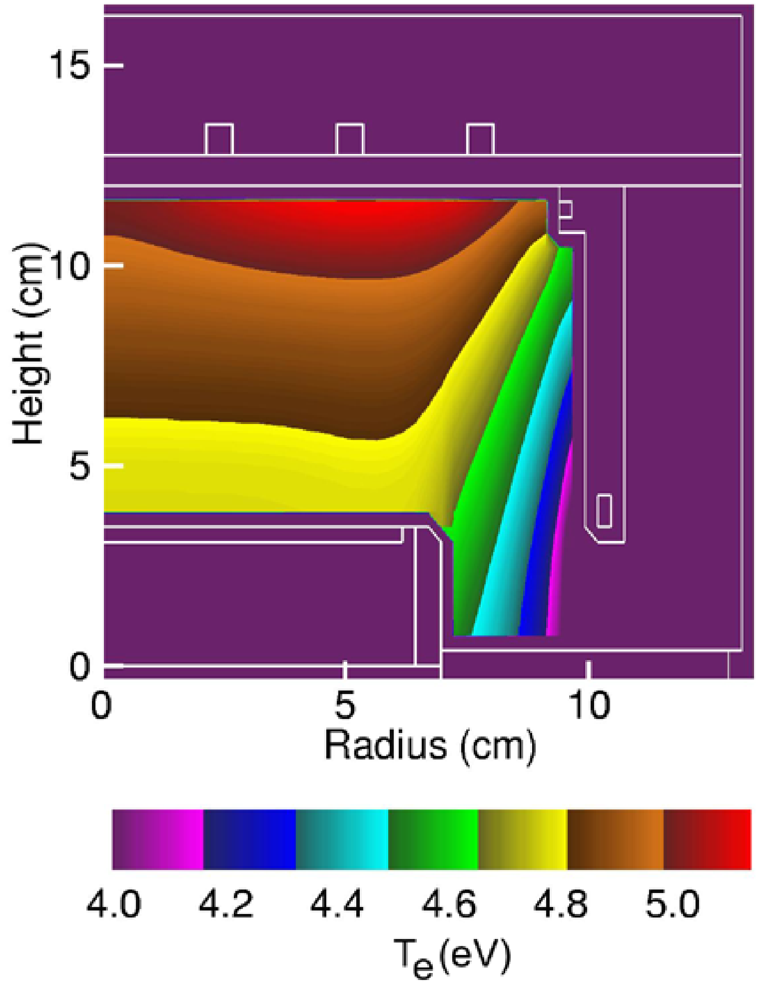

- C_4F_8, 10 mTorr, 1.4 kW, 13.56 MHz

University of Illinois
Optical and Discharge Physics

PROBE MEASUREMENTS OF ION SATURATION CURRENT

- **Ion saturation current in the case of low-pressure measurements is**

$$I_p = \frac{1}{4}\Delta\sqrt{\frac{2\pi T_e}{eT_i}}An_i q v_i$$ **Schott (1968)**

$$\Delta = \frac{r_s + r_p}{r_p}\left[erf\left(\frac{-\eta}{(r_s+r_p)^2/r_p^2 - 1}\right)^{1/2} + \frac{r_p}{r_s+r_p}\exp(-\eta)\left(1 - erf\left(\frac{-\eta(r_s+r_p)^2}{(r_s+r_p)^2 - r_p^2}\right)^{1/2}\right)\right]$$

where q = charge

n_i, v_i = ion density, ion thermal velocity

A = probe area

V_p = probe potential

η = qV_p/kT_i

T_i, T_e = ion, electron temperatures

r_s, r_p = sheath thickness, probe radius.

- **I_p is larger than the Langmuir current by $[2\pi T_e/(eT_i)]^{1/2}$ due to the pre-sheath.**

I_P FOR ICPs WITH MAGNETS IN Ar

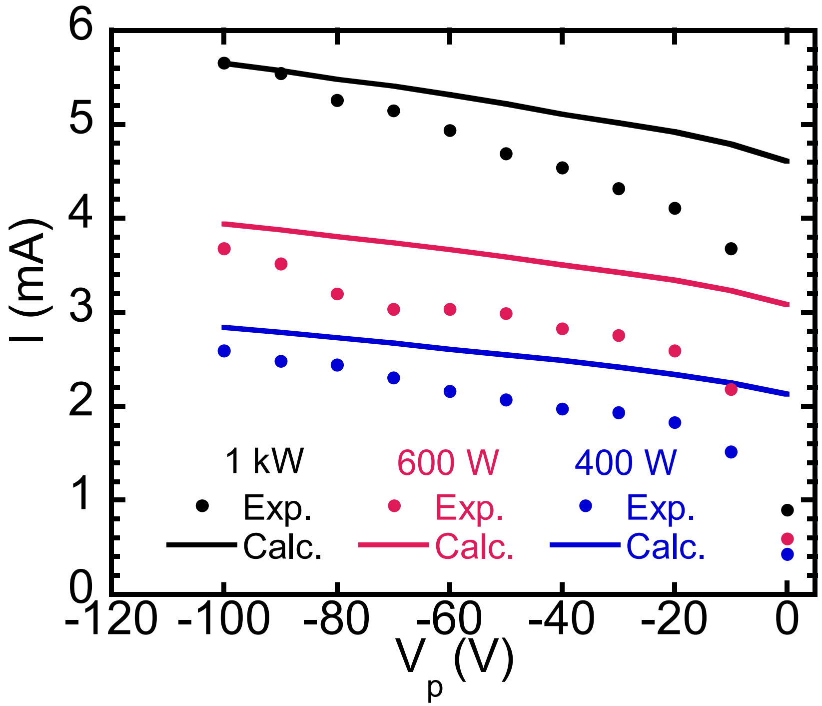

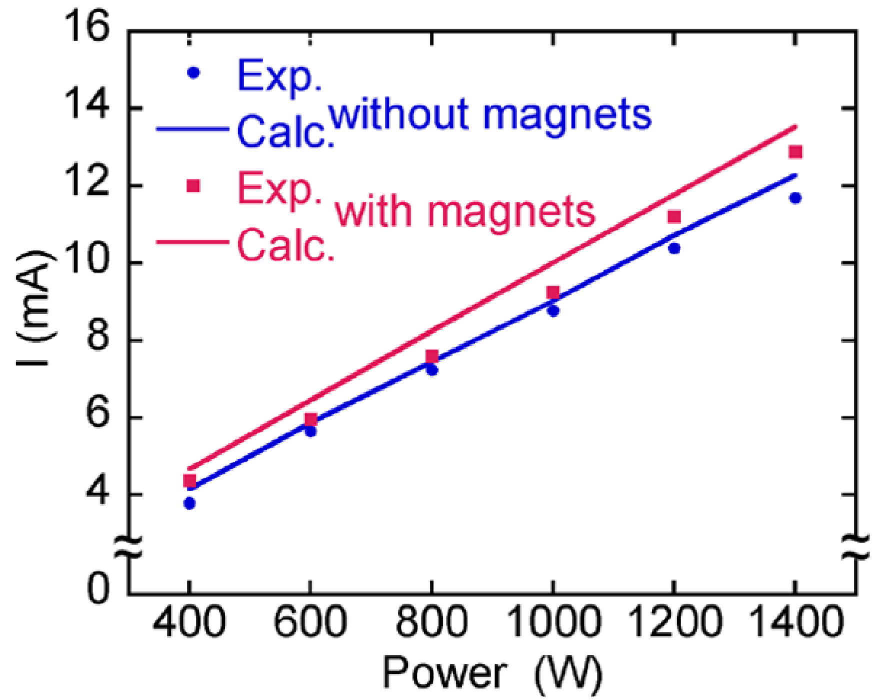

- Ion saturation current significantly varies with the probe collecting voltage.
- A linear dependence of ion saturation current on power is observed. (V_p=-100 V)

- Ar, 10 mTorr, 13.56 MHz

University of Illinois
Optical and Discharge Physics

I_P VERSUS POWER FOR ICPs IN O_2 AND C_4F_8

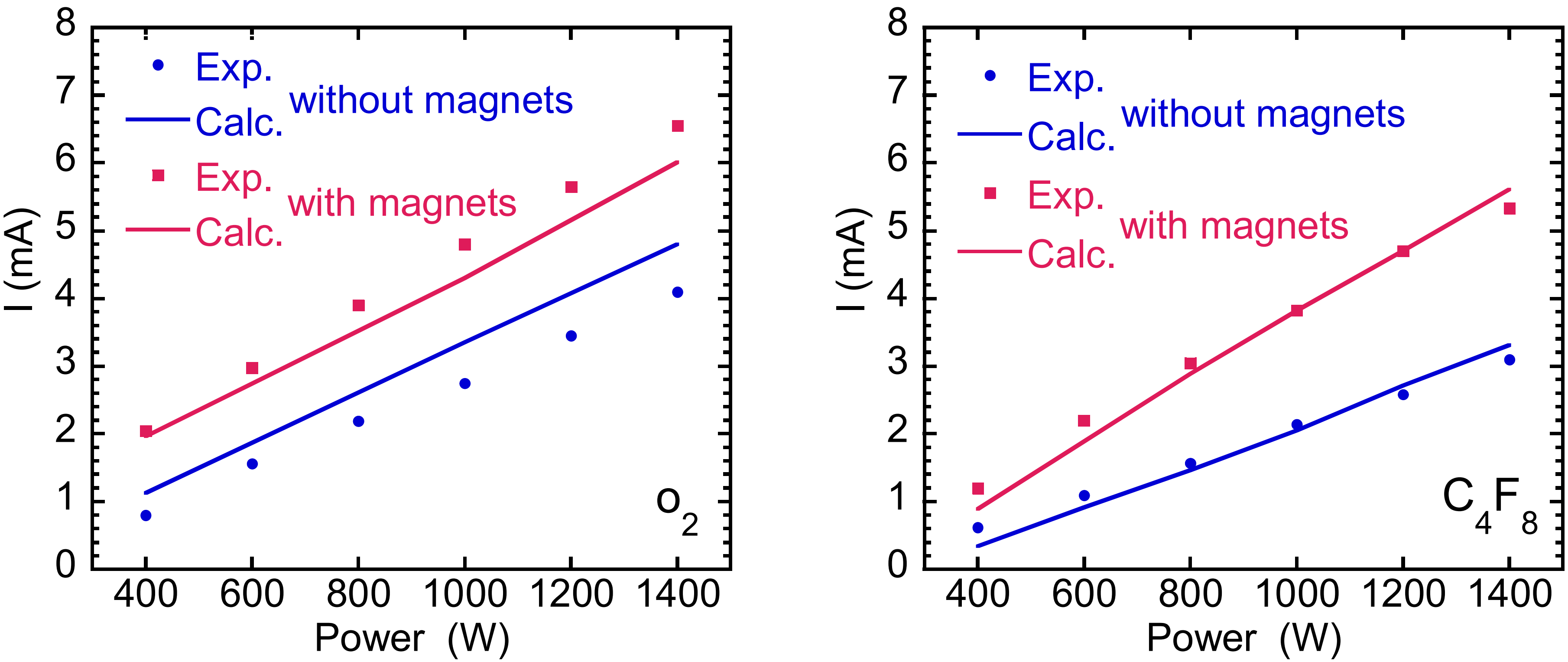

- **The ion saturation currents are larger if a static magnetic field is used to confine the plasma.**

- **Larger effects are seen in electronegative plasmas.**

- **10 mTorr, 13.56 MHz, 100 V probe bias.**

ION FLUXES FOR ICPs IN O_2

Experiment

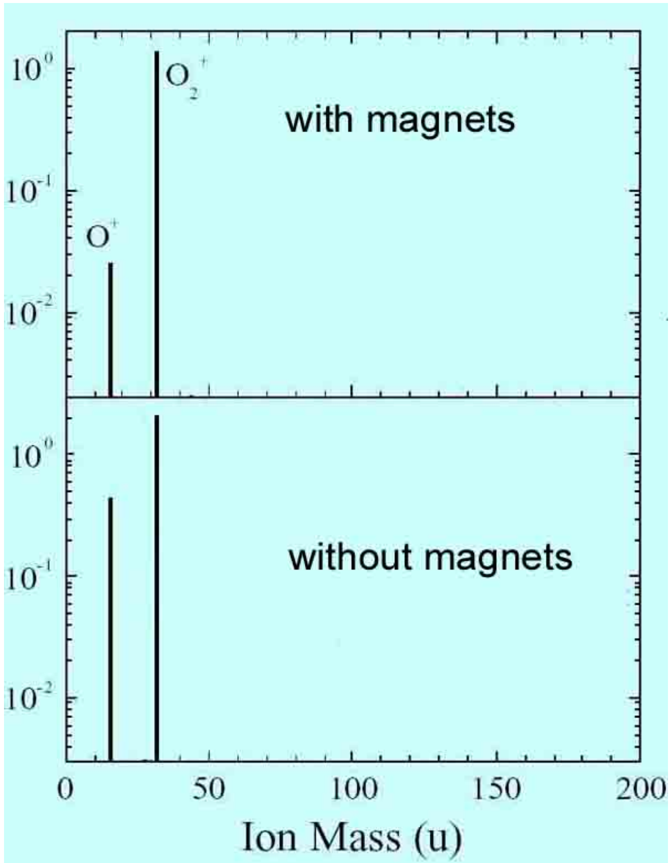

Model

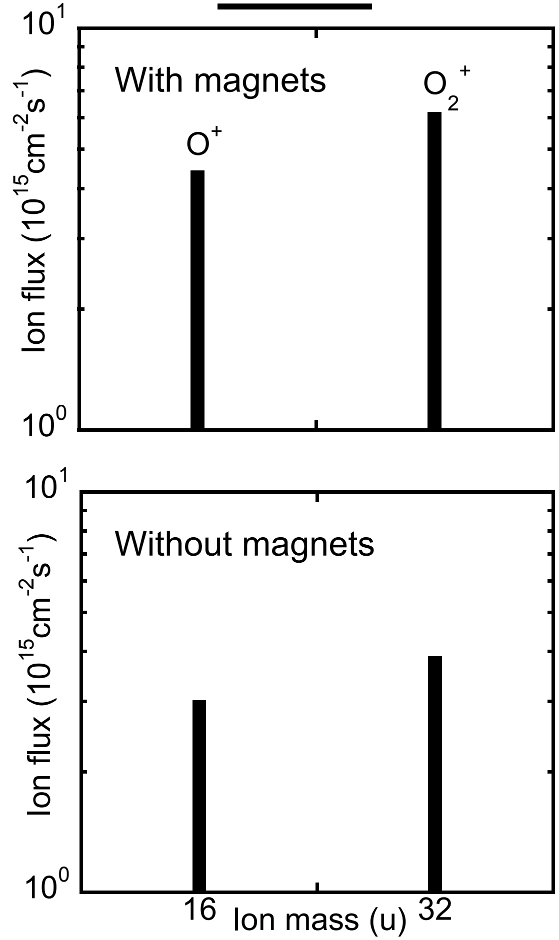

- **Smaller population of O^+ is observed in experiments.**
- **The model recombination coefficient for O on the walls may be too small.**

AVS_2002_15

- **O_2, 10 mTorr, 1kW, 13.56 MHz**

University of Illinois
Optical and Discharge Physics

IONS FLUXES FOR ICPs WITHOUT MAGNETS IN C_4F_8

Experiment

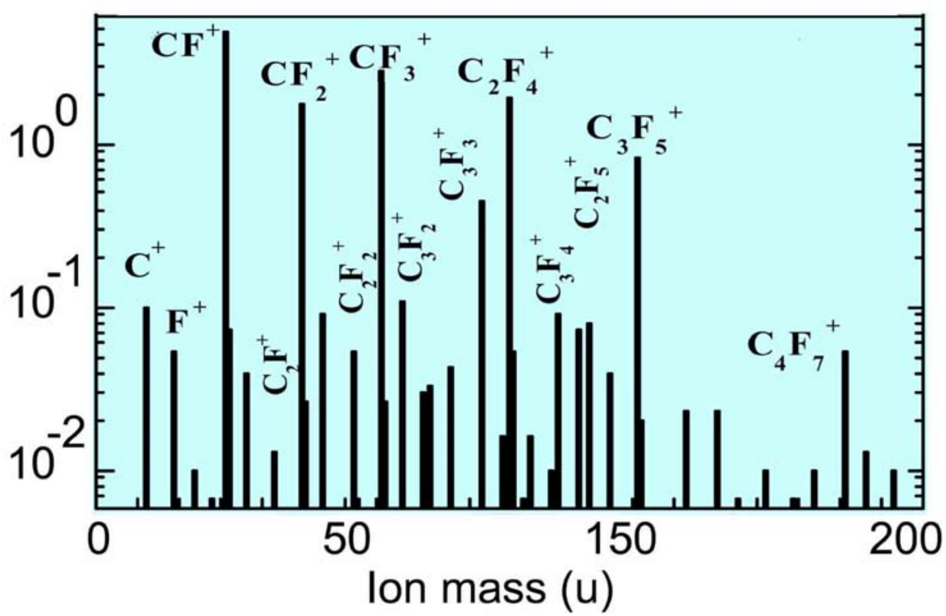

Model

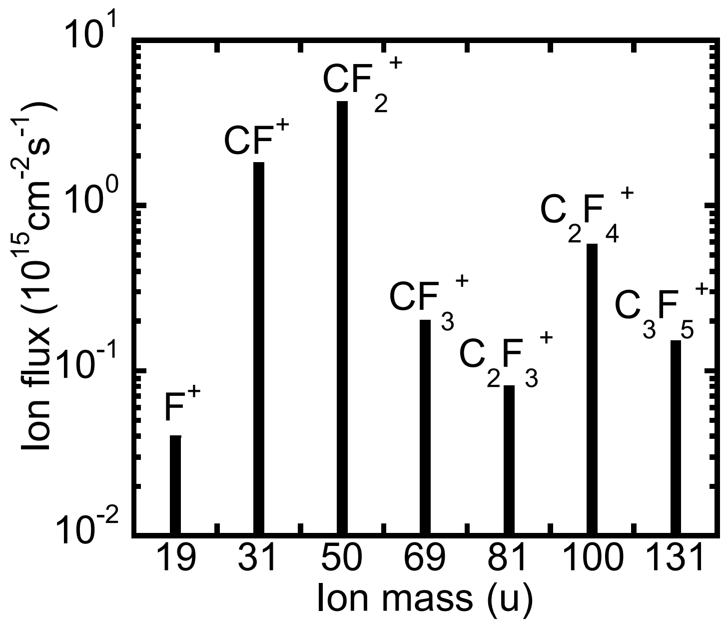

- **The model predicts the same set of dominant ions observed in experiments.**
- **The proportion of heavy ions is underestimated in the model, perhaps a consequence of improper initial branching or overestimated dissociation rates.**
- **C_4F_8, 6 mTorr, 600 W, 13.56 MHz**

University of Illinois
Optical and Discharge Physics

ION FLUXES FOR ICPs WITH MAGNETS IN C_4F_8

Experiment

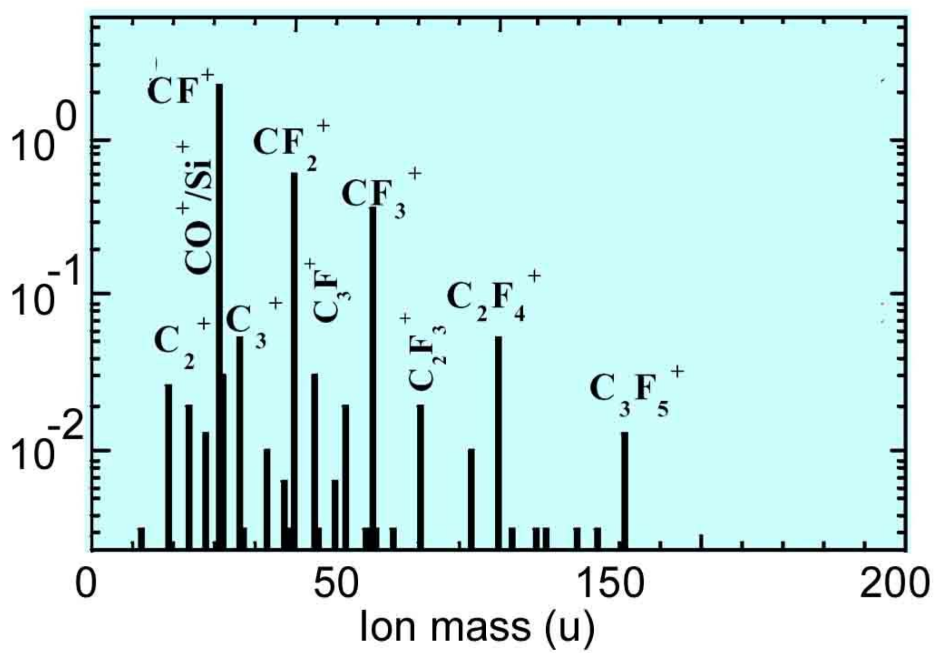

Model

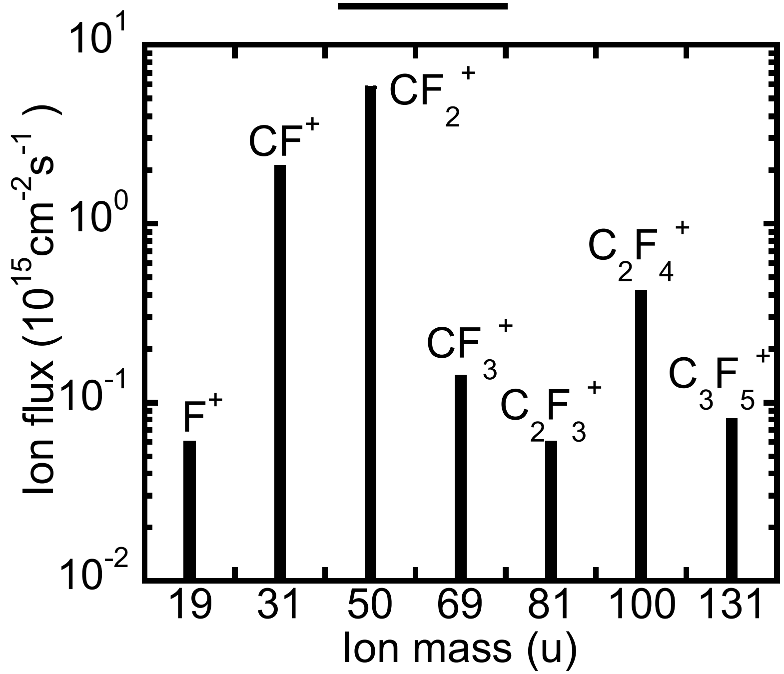

- **The ratio of heavy ion flux to light ion flux decreases with the use of the permanent magnets.**
- **Model underestimates [CF^+] and overestimates [$C_2F_4^+$].**
- **C_4F_8, 6 mTorr, 600 W, 13.56 MHz**

University of Illinois
Optical and Discharge Physics

EFFECT OF MAGNETS ON ELECTRON DENSITY

- **Without magnets electron density is largest in the middle of reactor where the electric potential is maximum.**

- **The static magnetic fields produce confinement in the periphery, increasing the electron density and flattening the plasma potential and [e].**

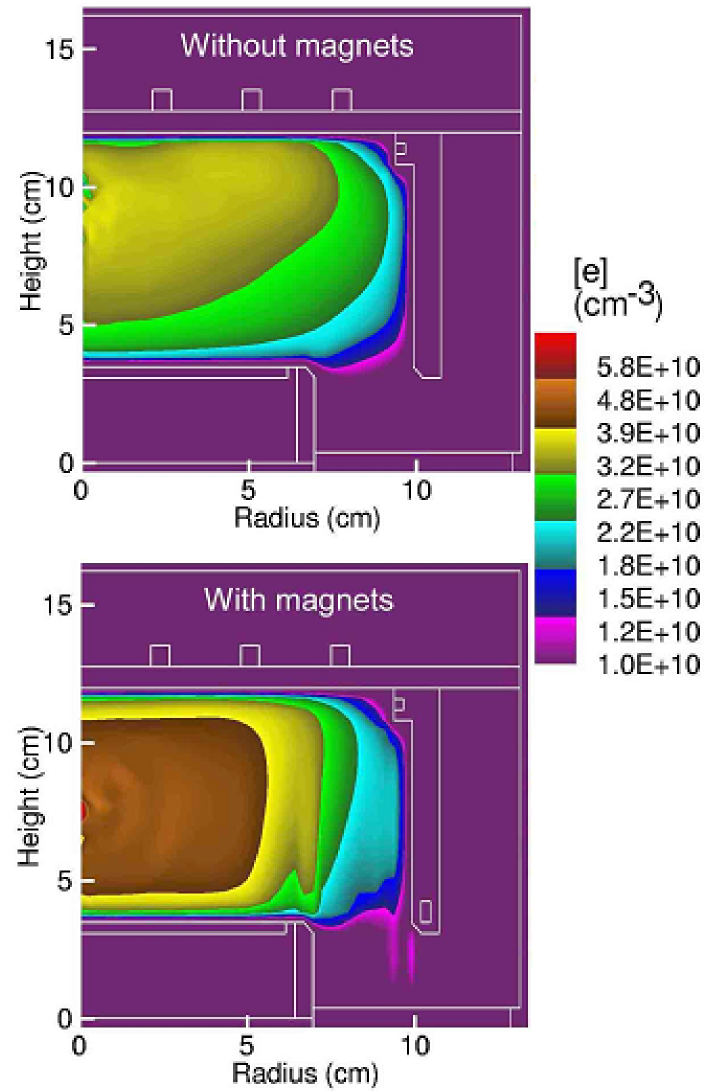

- **Ar/C_4F_8=20/80, 3 mTorr, 13.56 MHz, 400 W.**

University of Illinois
Optical and Discharge Physics

EFFECT OF MAGNETS ON [CF^+]

- **Without magnets [CF^+] has a maximum at the edge of the classical skin depth where the electron impact ionization is the largest.**

- **The static magnetic fields broaden the production of [CF^+] in the radial direction.**

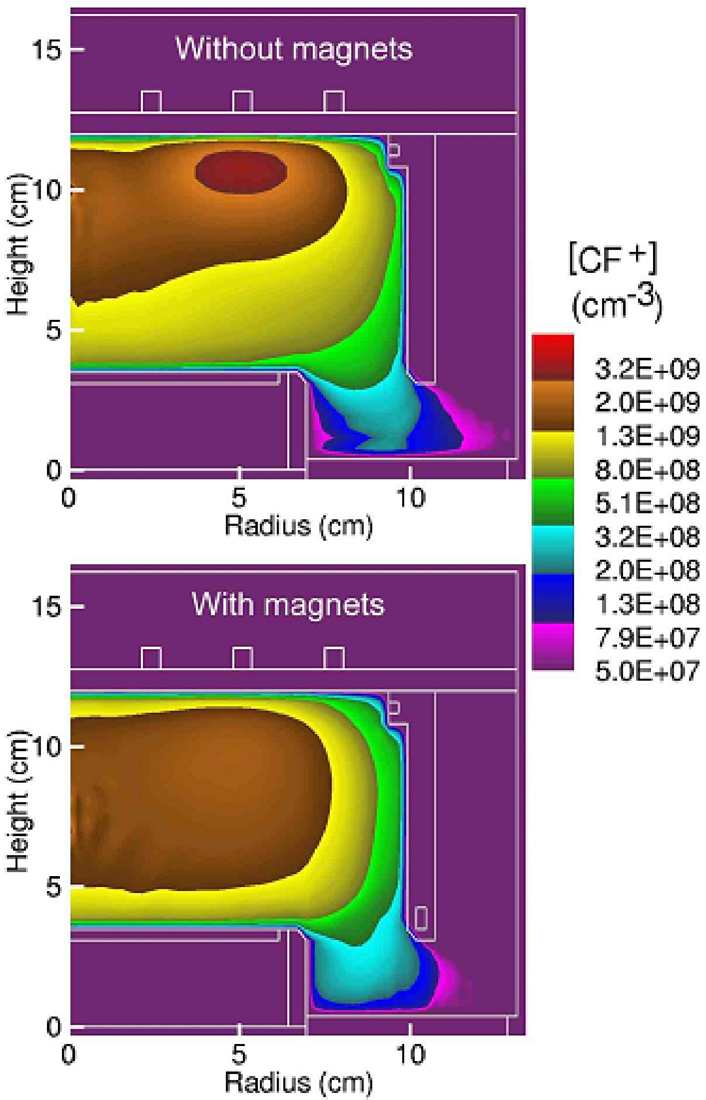

- **Ar/C_4F_8=20/80, 3 mTorr, 13.56 MHz, 400 W.**

University of Illinois
Optical and Discharge Physics

EFFECT OF MAGNETS ON ELECTRON TEMPERATURE

- **Without magnets the electron temperature is highest in the skin depth due to the collisionless electron heating.**

- **In the middle of the reactor the electrons are cooler because of the Ramsauer minimum in Ar elastic cross section and lack of efficient e-e heating.**

- **The static magnetic fields reduce the gradients in temperature due to the increase in the frequency of e-e collisions.**

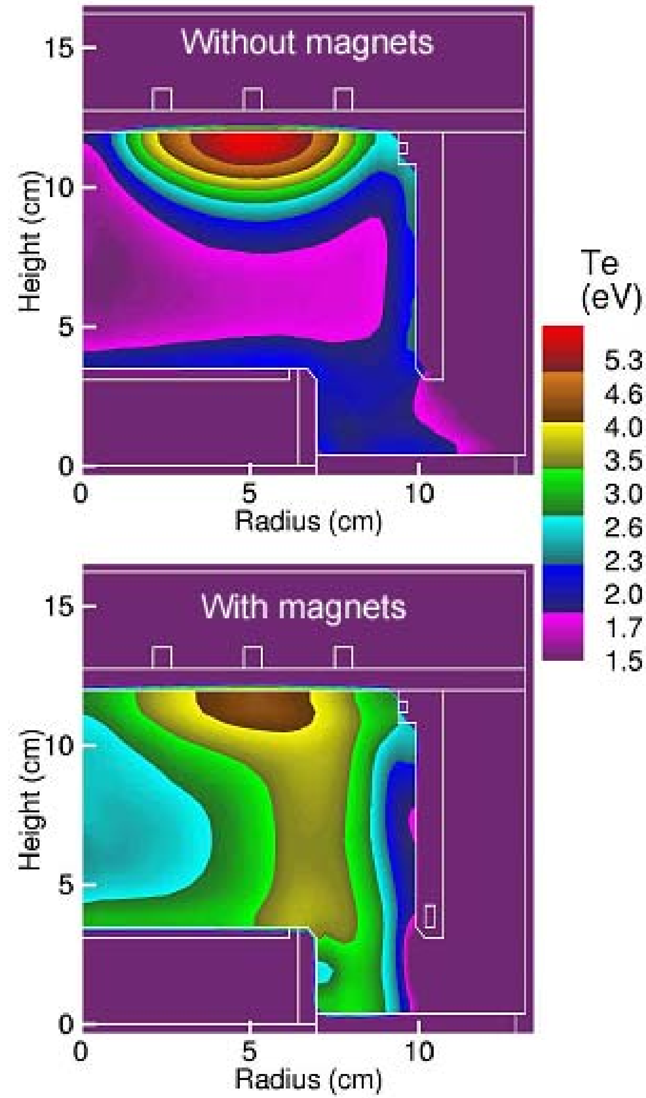

- **Ar/C_4F_8=20/80, 3 mTorr, 13.56 MHz, 400 W.**

University of Illinois
Optical and Discharge Physics

EEDs FOR ICP IN Ar/C_4F_8

- **Although the partial ionization is large, the electron energy distribution (EED) is non-Maxwellian as a result of the power being deposited in a non-uniform and non-linear fashion.**
- **The EEDs have long energy tails in the radial center of the skin layer due to collisionless heating.**
- **Low energy electrons "pool" at the peak in plasma potential in the center of the reactor.**

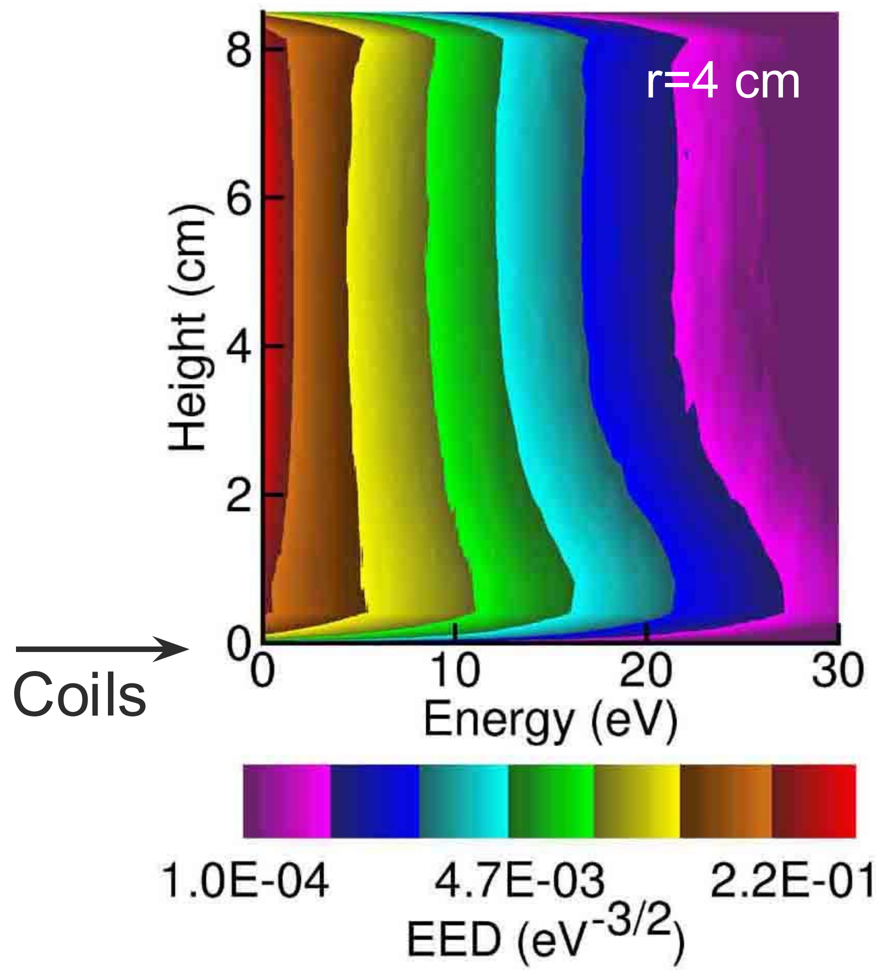

- **Ar/C_4F_8=20/80, 3 mTorr, 13.56 MHz, 400 W.**

University of Illinois
Optical and Discharge Physics

EFFECT OF MAGNETS ON POSITIVE POWER DEPOSITION

- **Without magnets the power is mainly deposited within the classical skin layer.**

- **The static magnetic fields increase the skin depth and the efficiency to deposit power within the plasma volume of interest.**

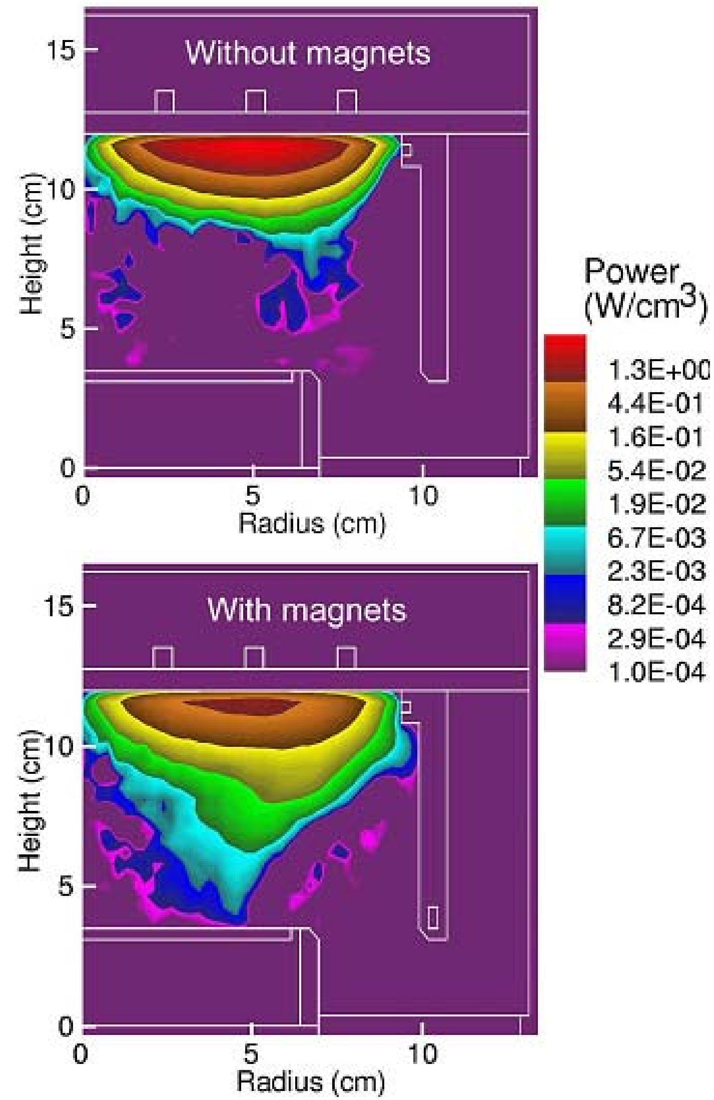

- **Ar/C_4F_8=20/80, 3 mTorr, 13.56 MHz, 400 W.**

University of Illinois
Optical and Discharge Physics

EFFECT OF MAGNETS ON NEGATIVE POWER DEPOSITION

- Negative power deposition results from noncollisional transport of electrons.
- Without magnets the major region of negative power deposition is close to the confinement ring due to the large electron flux directed toward the ring surface.
- The static magnetic fields decrease negative power deposition.

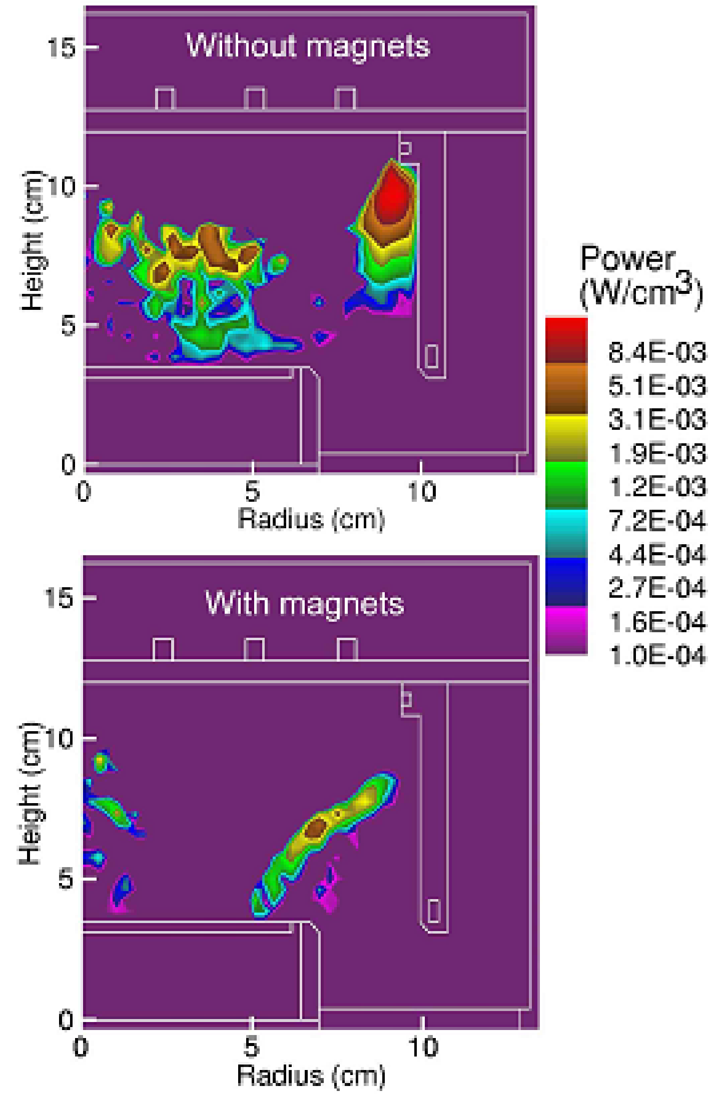

- Ar/C_4F_8=20/80, 3 mTorr, 13.56 MHz, 400 W.

University of Illinois
Optical and Discharge Physics

SUMMARY

- A new reaction mechanism for Ar/C_4F_8 was developed and validated against measured ion saturation currents obtained with probes and ion spectra measurements.

- The model predicts the same set of dominant ions observed in experiments.

- Static magnetic fields effectively confine the plasma and significantly increase the density of electrons and ions in the discharge.

- These fields also increase the skin depth and the efficiency to deposit power within the plasma volume of interest.

- In the skin layer the EED is far from Maxwellian distribution and it has the longest energy tail.

University of Illinois
Optical and Discharge Physics